An experimental and theoretical investigation of the triple fragmentation of CFClBr 2 by photolysis near 250 nm

ARTICLE *in* CHEMICAL PHYSICS LETTERS · MARCH 2003

Impact Factor: 1.9 · DOI: 10.1016/S0009-2614(03)00140-4

5 AUTHORS, INCLUDING:

Scott H Kable
University of New South Wales
148 PUBLICATIONS **2,294** CITATIONS
SEE PROFILE

Naomi L Haworth
Australian National University
29 PUBLICATIONS **459** CITATIONS
SEE PROFILE

George B Bacskay
University of Sydney
160 PUBLICATIONS **3,665** CITATIONS
SEE PROFILE

Available online at www.sciencedirect.com
SCIENCE DIRECT®
Chemical Physics Letters 370 (2003) 469–477
CHEMICAL PHYSICS LETTERS
www.elsevier.com/locate/cplett

An experimental and theoretical investigation of the triple fragmentation of $CFClBr_2$ by photolysis near 250 nm

Nathan L. Owens, Klaas Nauta, Scott H. Kable *, Naomi L. Haworth, George B. Bacskay

School of Chemistry, University of Sydney, Sydney, NSW 2006, Australia

Received 4 November 2002; in final form 13 January 2003

Abstract

Photodissociation of $CFClBr_2 + h\nu \rightarrow CFCl$ has been shown to occur for $\lambda < 274$ nm (436 ± 2 kJ mol^{-1}). G3 Ab initio calculations were performed to provide estimates of $\Delta_f H$ for $CFClBr_2$, CFClBr, and CFCl, which were calculated to be -188 ± 5, -43 ± 5 and $+30 \pm 5$ kJ mol^{-1}, respectively. The dissociation energies (0 K) for sequentially breaking the C–Br bonds were calculated to be 257 ± 5 and 183 ± 5 kJ mol^{-1}, respectively. The energy required to break both C–Br bonds was calculated to be 440 ± 5 kJ mol^{-1}, in excellent agreement with the experimental appearance threshold for CFCl. From the experimental appearance threshold, $\Delta_f H$ ($CFClBr_2$) is estimated to be -184 ± 5 kJ mol^{-1}.

1. Introduction

The role of halons and CFCs in the chemistry of the atmosphere has been well documented for many decades. As a general class of molecules, halomethanes absorb ultraviolet light via a $\sigma^* \leftarrow \sigma$ transition, which results in the cleavage of the weakest C–X bond (where X is halogen or hydrogen). The fate of the atom is very well understood and central to the depletion of stratospheric ozone. The fate of the halomethyl radical is less well understood, but the primary reaction is probably O_2 addition leading to the formation of halogen-substituted aldehydes and slow transport back to the troposphere [1].

Over the past couple of decades, several reports of UV or vacuum-UV excitation of halomethanes, resulting in cleavage of two C–X bonds, have appeared. Bromo- and iodomethane species seem to exhibit triple fragmentation pathways when the wavelength is shorter than 200 nm [2–9]. For wavelengths longer than 200 nm, however, only the difluoro-species, CF_2I_2, CF_2Br_2 and CF_2BrI have been reported to undergo triple fragmentation. CF_2I_2 undergoes a single C–I cleavage at longer wavelengths, which is believed to become two sequential C–I cleavages and finally concerted loss of two I-atoms as the energy of the dissociating photon is increased [9]. Triple fragmentation of CF_2Br_2 and CF_2BrI are also thought to be stepwise processes [4–8].

* Corresponding author.
E-mail address: s.kable@chem.usyd.edu.au (S.H. Kable).

0009-2614/03/$ - see front matter
doi:10.1016/S0009-2614(03)00140-4

In a series of papers on carbene spectroscopy we have created carbenes by photolysis of suitable halon precursors, for example CFCl from $CFClBr_2$ [10], and both CHF and CFBr from $CHFBr_2$ [11]. At the time, no attempt was made to elucidate the mechanism of carbene formation. In this Letter, we investigate the mechanism by which CFCl is formed from $CFClBr_2$ (halon-1112).

Interpretation of the results is made more difficult by the absence of thermochemical data concerning halon-1112. In fact, we could locate thermochemical data for only two dibromomethane compounds: CF_2Br_2 [12] and CH_2Br_2 [13]. The literature thermodynamic data for carbenes, including CFCl, are also highly varying. The most reliable current values are probably theoretical values obtained by Dixon et al. for CF_2 [14,15], CHBr and CBr_2 [16] and by Sendt and Bacskay [17] for CFCl. Both groups utilised the coupled cluster method with extrapolation to the complete basis limit and expect their results to be accurate to within ± 4 kJ mol^{-1}. The Gaussian-3 (G3) calculations of Sendt and Bacskay [17] for CF_2 and CFCl and the Gaussian-2 results of Cameron and Bacskay [12] for CHBr and CBr_2 are in good agreement with these coupled cluster results. More recently, the G3 procedure has been extended to be able to describe molecules containing atoms from the third row [18]. We have therefore calculated bond energies and heats of formation for a number of molecules with bromine using the G3 methodology. In addition to facilitating the interpretation of the experimental data, the calculations also permit us to test the accuracy of the G3 method for larger bromine-containing molecules, especially since the largest one in the G3 test set is CH_3Br.

The objectives of the current work are threefold. Firstly, we seek to establish whether there is a triple fragmentation pathway for $CFClBr_2$ following absorption of a single photon at stratospherically relevant wavelengths. Secondly, we use this data to determine thermochemical properties for the various species involved, including heats of formation and bond energies. Finally, we calculate those same thermochemical properties using the new formulation of G3 theory for third row atoms to verify both the experimental data and the validity of the theoretical method for larger bromine-containing compounds.

2. Experimental methods and results

2.1. Methodology

Details of the experiment can be found in our previous work on CFCl [10]. Briefly, helium (2 bar) was bubbled through $CFClBr_2$, (l, 0 °C) and expanded via a pulsed nozzle into a vacuum chamber. $CFClBr_2$ was photolysed at the nozzle orifice by a Nd:YAG pumped OPO (Coherent Infinity 40–100 and OPASCAN). The output of the OPO was varied from 480 to 560 nm and frequency doubled to yield light from 240 to 280 nm. The ensuing CFCl fragments were probed about 10 mm downstream, approx. 6 μs after the photolysis pulse, by an excimer pumped dye laser (Lambda Physik Lextra 200 and LPD 3001E, Exalite 398 dye). By allowing the CFCl to cool in the expansion, any effect of different CFCl product state distributions as a function of photolysis energy is negated. The trade-off in doing this is that the parent $CFClBr_2$ is fairly warm (we estimate 100–200 K).

Fluorescence from CFCl was imaged onto the slits of a Spex Minimate monochromator with 5 mm slits, which acts like a 20 nm triangular bandpass filter. This filter provides no real rotational or vibrational resolution for the CFCl fluorescence. The broadband fluorescence was detected by an EMI 9789QB photomultiplier, the signal passed to an SRS-250 boxcar averager and finally to an SRS-245 A/D board and a personal computer. The experiment was timed using the internal variable delays provided by the Infinity laser.

2.2. Results

An absorption spectrum of $CFClBr_2$, diluted in air, measured on a Cary 4E spectrometer, is shown in Fig. 1 (top). The spectrum shows negligible absorption in the actinic range ($\lambda > 295$ nm) and no sharp features, which is typical of halon and CFC species. At least two broad overlapping

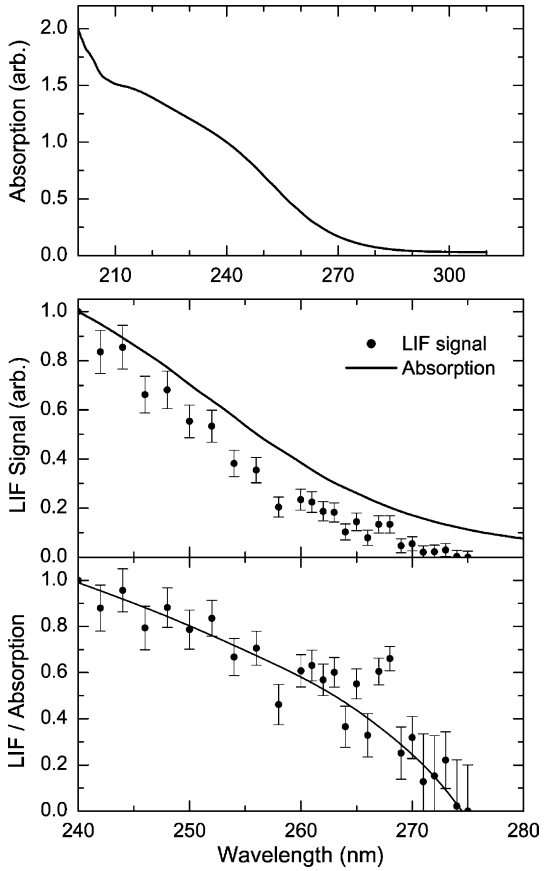

Fig. 1. (Top) $CFClBr_2$ absorption spectrum; (centre) photofragment excitation spectrum of $CFClBr_2$; (bottom) ratio of photofragment LIF signal to absorption signal. The solid line is a spline fit to the data to indicate the trend. The threshold to CFCl formation is indicated by where the ratio curve cuts the x-axis near 274 nm.

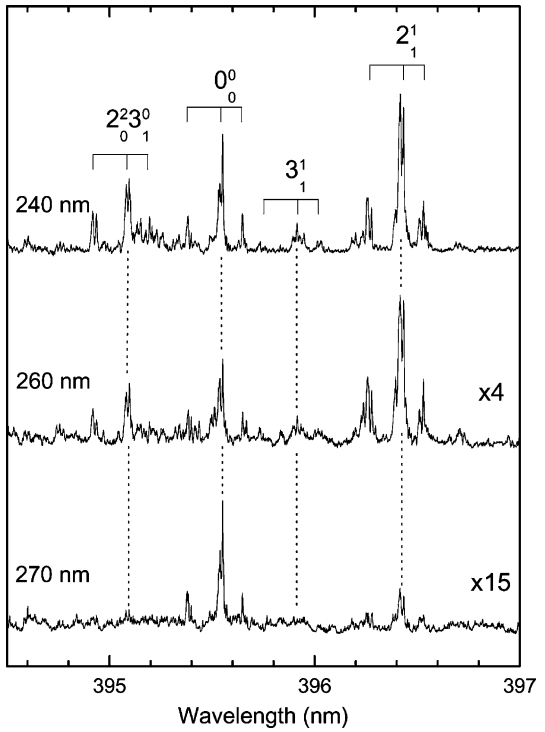

Fig. 2. CFCl fluorescence excitation spectra in the origin region following dissociation in $CFClBr_2$ at 240, 260 and 270 nm. Indicated at the top are the vibronic assignments with sticks to indicate the dominant rotational structure.

features are evident, the one to the red (around 240 nm) forming a pronounced shoulder on the stronger feature to the blue, which peaks further to the blue than the range of the spectrometer. By analogy with other CFCs and halons, such features are likely to be $\sigma^* \leftarrow \sigma$ transitions involving a C–Br bond.

The photolysis of $CFClBr_2$ is known to result in the formation of CFCl [10]. Several LIF spectra of CFCl produced in this way are shown in Fig. 2. The origin region is shown, which is quite weak due to poor Franck–Condon overlap with the ground state. However, it is relatively uncongested, least affected by chlorine isotopic features, and also has well-assigned hot bands and so we have concentrated on this region. The spectral features pertinent to this work are the origin transition, and a variety of hot-band transitions emanating from the $v_2 = 1$ and $v_3 = 1$ levels ($v_2 =$ bend, $v_3 =$ C–Cl stretch). The main rotational sub-branches are indicated by a comb. The main feature is the strong $^{r}Q_0$ sub-branch, flanked by the $^{r}Q_1$ to shorter wavelength and the $^{p}Q_1$ to longer wavelength. The reader is referred to previous work on CFCl spectroscopy [10] for any further details.

The mechanism of CFCl production from $CFClBr_2$ was not explored previously. The first test that was performed was to establish the dependence of the CFCl signal on pump laser power. The LIF signal from the central peak of the 0_0^0 transition was monitored as the pump power was

varied randomly. The resulting dependence is shown in Fig. 3 and indicates that the observed signal varies linearly with laser power.

The LIF intensity from the 0_0^0 transition was also monitored as the pump wavelength was changed randomly between 240 and 275 nm as shown in Fig. 1 (centre). The data points in the figure arise from about 1000 laser shots and were taken every 2 nm below 260 nm and then every 1 nm above 260 nm. For comparison, the absorption spectrum is also plotted on the same axes, arbitrarily normalised to the value at 240 nm. The shapes of the two spectra are similar, but the excitation spectrum rises more rapidly towards 240 nm than does the absorption spectrum. Additionally, the excitation spectrum has reached zero (no CFCl observed) at 275 nm while the absorption spectrum is still about 10% of the 240 nm value and, as shown in the top panel, continues well beyond 280 nm. The actual wavelength at which the excitation spectrum reaches zero is rather difficult to determine in this spectrum as the data converge asymptotically to zero over about 5 nm.

The difference between the excitation and absorption spectrum is accentuated in Fig. 1 (bottom) by plotting the ratio of the excitation to absorption intensity. Quite clearly, relative to the absorption spectrum, the intensity of the excitation spectrum drops consistently from 240 to 260 nm and then drops quite sharply towards 275 nm. The line is a heavily smoothed spline fit, which cuts the abscissa at 274 nm and we estimate the threshold for production of CFCl from $CFClBr_2$ to be 274 ± 2 nm, which corresponds to a photon energy of $36{,}500 \pm 280$ cm^{-1}.

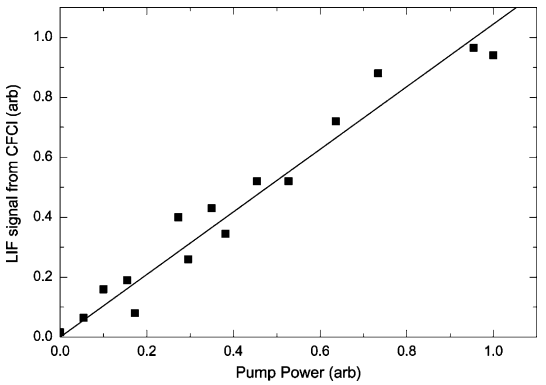

Fig. 3. Power dependence of the CFCl signal following dissociation of $CFClBr_2$ at 240 nm.

More information about the threshold can be obtained by examining the CFCl spectrum as a function of wavelength. Three such spectra are shown in Fig. 2, obtained following excitation of $CFClBr_2$ at 240, 260 and 270 nm. The 240 nm spectrum was discussed earlier and shows features arising from population in $\upsilon = 0$, $\upsilon_2 = 1$ and $\upsilon_3 = 1$, which have vibrational energies of 0, 447 and 753 cm^{-1}, respectively [10]. Although the 2_1^1 transition is strongest, the Franck–Condon factor for the 2_1^1 transition is about 15 times larger than the 0_0^0 transition [10] so the population in the $\upsilon_2 = 1$ level is actually about an order of magnitude less than in $\upsilon = 0$. The 3_1^1 Franck–Condon factor is similar to 0_0^0 [10] and therefore the $\upsilon_3 = 1$ population is also much less than $\upsilon = 0$.

At 260 nm the relative population in these vibrational levels has not changed much, although the overall signal is reduced by a factor of about four. The 270 nm spectrum, however, shows CFCl population only in the $\upsilon = 0$ and $\upsilon_2 = 1$ levels, with the 0_0^0 transition dominant. The overall signal is now about 15 times reduced in comparison with the 240 nm spectrum.

The data above are summarised in Fig. 4. A photon energy of 36,360 cm^{-1} (275 nm) does not lead to detectable CFCl. At 37,037 cm^{-1} (270 nm) CFCl in the $\upsilon = 0$ and $\upsilon_2 = 1$ states are produced and at 38,460 cm^{-1} (260 nm), $\upsilon = 0$, $\upsilon_2 = 1$ and $\upsilon_3 = 1$ levels are populated. The energy level diagram shows that all three observations are satisfied if the combined dissociation energy for both C–Br bonds is $36{,}475 \pm 120$ cm^{-1}. This is in good agreement with the threshold from the excitation spectrum of Fig. 1, which was $36{,}500 \pm 280$ cm^{-1}.

There are two concerns at this stage from proclaiming this to be an unambiguous experimental measurement of the threshold to triple fragmentation of $CFClBr_2$: (i) the observation of a linear power dependence for CFCl production is a necessary but not sufficient condition for the process to be single photon, and (ii) we have not addressed the possibility that CFCl is produced in concert with a Br_2 molecule, rather than two Br atoms.

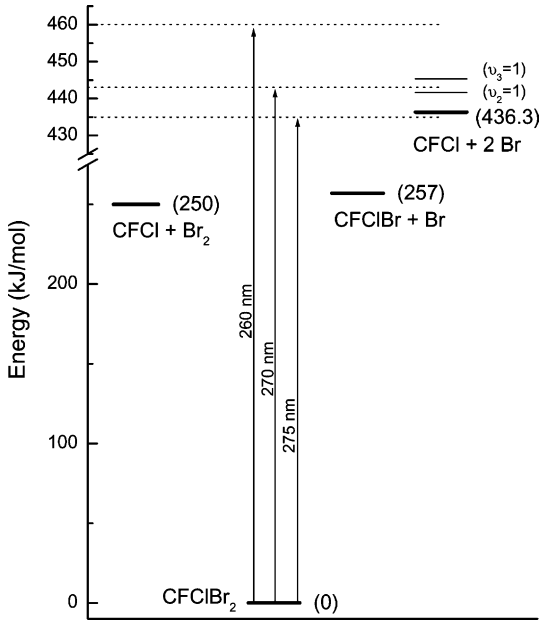

Fig. 4. Energy level diagram of $CFClBr_2$ and various reaction products calculated in this work. The energies in parentheses are based on theoretical calculations in this work, except for the CFCl + 2Br channel which is our experimental value.

These issues could be resolved by detailed consideration of the thermochemistry of the appropriate processes. In the absence of reliable heats of formation for $CFClBr_2$ or CFClBr we have carried out high level ab initio calculations of these properties, which are presented in the next section. The theoretical and experimental data are tied together to resolve these issues in Section 4.

3. Theoretical methods and results

The G3 procedure for molecules with third row atoms has only been developed very recently. The method is essentially the same as that initially proposed for first and second row atoms [19], where the energy of a hypothetical QCISD(T) calculation with a large basis set is approximated by performing such a calculation with a significantly smaller basis set, followed by corrections for enlargement of the basis set, which are computed at lower levels of theory, namely MP2 and MP4. The G3 energy can be summarised as

$$
\begin{aligned}
&E_0[\mathrm{G3}] \\
&\quad = E[\mathrm{QCISD(T)/6\text{-}31G(d)}] \\
&\qquad + \{E[\mathrm{MP4/6\text{-}31+G(d)}] \\
&\qquad - E[\mathrm{MP4/6\text{-}31G)(d)}]\} \qquad (+\text{correction}) \\
&\qquad + \{E[\mathrm{MP4/6\text{-}31G(2df,p)}] \\
&\qquad - E[\mathrm{MP4/6\text{-}31G)(d)}]\} \qquad (2\mathrm{df,p\ correction}) \\
&\qquad + \left\{ \begin{array}{l} E[\mathrm{MP2(Full)/GTLarge}] \\ -E[\mathrm{MP2/6\text{-}31G(2df,p)}] \\ -E[\mathrm{MP2/6\text{-}31+G(d)}] \\ +E[\mathrm{MP2/6\text{-}31G(d)}] \end{array} \right\} \ (\mathrm{G3Large\ correction}) \\
&\qquad + \Delta E_{\mathrm{ZPE}} + \Delta E_{\mathrm{SO}} + \Delta E_{\mathrm{hlc}},
\end{aligned}
$$

where the appropriate corrections due to successive basis set enlargement are evaluated at the MP4 and MP2 levels of theory. ΔE_{ZPE} is the zero point vibrational energy, ΔE_{SO} denotes spin–orbit coupling corrections and ΔE_{hlc} is an (empirical) higher level correction.

The geometry and zero point vibrational energy are determined at the MP2(Full)/6-31G(d) and HF/6-31G(d) levels of theory, respectively. Note that the G3 formulation for third row atoms recommends the use of a new set of basis functions [18], which are based on the 6-31G basis of Rassolov et al. [20]. As for first and second row atoms, the G3 calculations on molecules containing third row atoms are performed with six d and seven f functions, except in the case of G3Large calculations, which utilise the spherical harmonic representation for all orbitals, viz. (5d, 7f). Furthermore, following the work of Duke and Radom [21], who noted an improvement in the accuracy of the G2 procedure when the 3d electrons of third row atoms were unfrozen to correlation, the G3 procedure also prescribes the inclusion of the 3d orbitals of third row atoms in the valence space.

Once G3 absolute energies have been calculated, atomisation energies and thus heats of formation can be calculated using the relevant (experimental) atomic data. Heats of formation can also be determined on the basis of reaction enthalpies, preferably those of isodesmic reactions where the number of bonds of each type are conserved in the reaction. Errors in the theoretical description of a particular atom or bond are then expected to cancel, resulting potentially in a rela-

Table 1
Energies, atomisation energies and heats of formation (at 0 and 298 K) (kJ mol^{-1} unless otherwise noted)

Species	E_0/E_h	AE	$\Delta_f H^0$ (0 K)[a]	$\Delta_f H^0$ (298 K)			Ref.
	G3	G3	G3	G3/AE[a]	G3/ID[b]	Experimental	
$CFClBr_2$	−5745.04026	1319.2	−187.4	−188.2	−190.6	-184 ± 5	This work
CFClBr	−3171.42502	1062.5	−42.5	−42.9			
CFCl	−597.83777	879.2	28.9	29.8		31 ± 13	[24]
Br_2	−5147.10746	190.4	33.3	34.6		30.91 ± 0.11	[23]
Br	−2573.51747					111.87 ± 0.12	[23]
CH_3Br	−2613.41950	1500.0	−28.9	−36.1		-34.2 ± 0.8	[25]
						-36 ± 1	[26]
CH_4	−40.45762	1643.3	−68.0	−75.9		−74.87	[23]
CH_2F_2	−238.86226	1743.6	−445.8	−453.4		−450.66	[23]
CH_3Cl	−499.91301	1552.5	−73.6	−81.5		−83.68	[23]
CH_2Cl_2	−959.37121	1469.2	−86.7	−93.5		−95.52	[23]
CF_4	−437.30780	1951.4	−931.1	−936.8		-933.04 ± 0.7	[27]

[a] Heat of formation calculated from atomisation energies.
[b] Heat of formation calculated by isodesmic schemes.

tively accurate estimate of the heat of the reaction. Application of Hess' law then allows the determination of the heat of formation of a given species, provided accurate (experimental) heats of formation are available for all other species in the reaction. Isodesmic reaction schemes have been used in this work to confirm the reliability of the heats of formation obtained from G3 atomisation energies.

The quantum chemical computations were carried out using the GAUSSIAN 98 suite of programs [22] on DEC alpha 600/5/333 and COMPAQ XP100/500 workstations of the Theoretical Chemistry group at the University of Sydney and on the COMPAQ AlphaServer SC system of the Australian Partnership for Advanced Computing National Facility at the National Supercomputing Centre, ANU, Canberra.

The computed G3 total energies, atomisation energies and heats of formation at 0 and 298 K are reported in Table 1. The absolute energies of Br_2, Br and CH_3Br have been reported earlier by Curtiss et al. [18]. As they did not report the atomisation energies or heats of formation of Br and CH_3Br, we have generated this additional data and include it here for completeness. The G3 results for CFCl, CH_4, CH_2F_2, CH_3Cl, CH_2Cl_2 and CF_4 have also been published previously but are quoted here because of their importance in the decomposition reactions of $CFClBr_2$ and in the isodesmic reaction schemes.

Table 2 lists the various isodesmic reactions which were employed to determine the heat of formation of $CFClBr_2$ from the G3 reaction energies, along with the resulting enthalpies of formation. The spread of values about the mean is less than 4 kJ mol^{-1}, suggesting chemical accuracy in the results. The average value obtained by this approach differs by only 2.4 kJ mol^{-1} from the heats of formation obtained from the G3 atomisation energies, which is well within the expected uncertainties of the G3 calculations. This suggests that the G3 procedure is indeed capable of producing accurate heats of formation from atomisation energies for larger third row containing molecules and therefore the use of isodesmic schemes is not warranted.

Table 2
Isodesmic reaction schemes and resulting G3 enthalpies of formation for $CFClBr_2$ (kJ mol^{-1})

Reaction	$\Delta_f H^0$ (298 K)
$2CFClBr_2 + 4CH_4 \rightarrow CH_2F_2 + CH_2Cl_2 + 4CH_3Br$	−190.5
$2CFClBr_2 + 5CH_4 \rightarrow CH_2F_2 + 2CH_3Cl + 4CH_3Br$	−192.2
$2CFClBr_2 + 3CH_4 + CH_2F_2 \rightarrow CH_2Cl_2 + 4CH_3Br + CF_4$	−190.9
$2CFClBr_2 + 3CH_4 + 2CH_3Cl \rightarrow 2CH_2Cl_2 + 4CH_3Br + CH_2F_2$	−188.9
Average for $CFClBr_2$	−190.6

4. Discussion

The experimental data demonstrate conclusively that CFCl is a by-product of $CFClBr_2$ photolysis and that the process is likely to involve the absorption of only one photon. The threshold for CFCl production was found to be 436 ± 2 kJ/mol or $36{,}475 \pm 120$ cm^{-1}. CFCl can be formed from $CFClBr_2$ by two different reactions:

$$CFClBr_2 \xrightarrow{h\nu} CFCl + Br_2 \quad (1)$$

$$CFClBr_2 \xrightarrow{h\nu} CFCl + 2Br \quad (2)$$

The observed appearance threshold for CFCl could correspond to either of these reactions. A schematic of the chemical energies involved in each process is shown in Fig. 4. The left-hand side of the figure shows the Br_2 production, while the right-hand side shows sequential or concerted elimination of two Br atoms. To help distinguish between these two reactions we turn to the ab initio results from above.

The G3 method has provided estimates of the heats of formation ($\Delta_f H$) for all species involved in this work. The heats of formation of Br and Br_2 are well known [23]. All $\Delta_f H$ data are reported in Table 1, which were then used to evaluate the reaction energy for various reactions, as shown in Table 3. The calculated energy required for reaction (1) is 250 ± 5 kJ/mol and for reaction (2) is 440 ± 5 kJ/mol. The value for reaction (2) is comfortably within the mutual error limits for the theoretical and experimental estimates. This does not absolutely discount reaction (1) because as a three-centre elimination it would probably require a barrier. However, it would seem too fortuitous that the barrier height is exactly the same as the thermochemical threshold for the other channel. Therefore, we have rejected the three-centre elimination pathway as much less likely than the triple fragmentation pathway. These conclusions are also in accord with the analogous findings for the CF_2Br_2 [7] and CF_2BrI molecules [4].

Table 3
Reaction energies for possible decomposition pathways for $CFClBr_2$ (kJ mol^{-1})

Reaction	$\Delta_r E$ (0 K) G3	$\Delta_r H$ (298 K) G3
$CFClBr_2 \rightarrow CFCl + 2Br$	439.9	441.7
$CFClBr_2 \rightarrow CFClBr + Br$	256.7	257.2
$CFClBr \rightarrow CFCl + Br$	183.2	184.5
$CFClBr_2 \rightarrow CFCl + Br_2$	249.5	252.6

Since $\Delta_f H$ is known for CFCl and Br we can use the threshold energy to determine an experimental heat of formation for $CFClBr_2$. The value so determined is $\Delta_f H\ (0\ K) = -183.4 \pm 5$ kJ mol^{-1} (using the G3 value for CFCl as the experimental value is quite uncertain). The G3 method also provides heat capacity correction factors between 0 and 298 K. For $CFClBr_2$ this difference is 0.8 kJ mol^{-1}, which provides an estimate for $CFClBr_2$ of $\Delta_f H\ (298\ K) = -184.2 \pm 5$ kJ mol^{-1}. The G3 values are in excellent agreement with this experimental heat of formation.

The triple fragmentation reactions of several halomethane species containing Br and I have been reported previously. Most of the experiments have been carried out in the far or vacuum ultraviolet region ($\lambda < 200$ nm), which typically excites the second absorption band (see Fig. 1 for this band in $CFClBr_2$). For example CF_2BrCl [2], CF_2BrI [4], CH_2BrI [3], CF_2Br_2 [3–8] and CF_2I_2 [9] have all been reported to exhibit competing chemical channels, cleaving one or other of the C–Br or C–I bonds (if different), and for cleavage of both bonds. Chloro- and fluoromethane species (containing no Br or I), conversely, do not show triple fragmentation (involving C–Cl cleavage), at least down to 193 nm.

The mechanism for the triple fragmentation of halomethanes is not assured with some studies favoring a concerted triple whammy, while others favour the formation of a hot halomethyl radical intermediate, followed by spontaneous dissociation into the carbene. The problem is that, although the spectra of these species appear simple, there are actually several electronic transitions that contribute to each 'peak' in the spectrum. To our knowledge, there has been no definitive theoretical study of a bromo- or iodomethane species where one of these states has been shown to correlate with concerted triple fragmentation. In the absence of theoretical assistance experimentalists rely on the nuances of the atom recoil energy distributions

to try and decide between concerted and stepwise mechanisms.

In the first electronic absorption band of bromomethane species there is fairly uniform agreement that a $\sigma^* \leftarrow \sigma$ transition localised on a C–Br bond is excited, which leads to formation of Br plus a halomethyl radical with quantum yields approaching unity. Only two other bromomethanes have been reported to undergo triple fragmentation within this band, namely CF_2BrI [3] and CF_2Br_2 [4,8]. The work on CF_2Br_2 has been quite extensive over a couple of decades and the consensus now seems to be that CF_2Br_2 undergoes triple fragmentation for wavelengths shorter than 260 nm. At these wavelengths the primary process is still the breaking of one C–Br bond. The resultant CF_2Br radicals are born with a wide range of internal energy, some having sufficient energy for spontaneous decomposition into $CF_2 + Br$. The experimental data for $CFClBr_2$ bear a striking similarity to CF_2Br_2, which lead us to suspect that the mechanism of triple fragmentation is probably the same, i.e., direct loss of one Br atom, followed by spontaneous loss of the second Br atom from a hot intermediate CFClBr radical.

5. Conclusions

In this work, we have established that CFCl is formed from single photon dissociation of $CFClBr_2$ for wavelengths shorter than 274 nm. We attribute this to a thermochemical threshold, and hence determine the energy required to break both C–Br bonds to be 436 ± 2 kJ mol^{-1}. Ab initio calculations using the G3 method confirm that two bromine atoms are the partners in this reaction. The heat of formation of $CFClBr_2$ is inferred from these experiments to be $\Delta_f H(298\ \mathrm{K}) = -184 \pm 5$ kJ mol^{-1}, in excellent agreement with the computed G3 value of -188 ± 5 kJ mol^{-1}. These ab initio calculations are the first reports of dibromo species at the G3 level. Comparison of the heat of formation by G3 calculation with that calculated from the average value from a set of isodesmic reactions shows agreement to within 2.4 kJ mol^{-1}, thereby confirming the reliability of the G3 method for these species.

Acknowledgements

We express our thanks to the Australian Research Council (Project A10009325) for supporting this research and the Australian Partnership for Advanced Computing National Facility for access to the COMPAQ AlphaServer SC system. We thank Mr. Joseph Guss for helping to set up the experiment. N.L.H. gratefully acknowledges the award of an Australian Postgraduate Research Scholarship.

References

[1] B.J. Findlayson-Pitts, J.N. Pitts Jr., Atmospheric Chemistry: Fundamentals and Experimental Techniques, Wiley, New York, 1986.
[2] G. Baum, J.R. Huber, Chem. Phys. Lett. 213 (1993) 427.
[3] L.J. Butler, E.J. Hintsa, S.F. Shane, Y.T. Lee, J. Chem. Phys. 86 (1987) 2051.
[4] P. Felder, X. Yang, G. Baum, J.R. Huber, Isr. J. Chem. 34 (1993) 33.
[5] T.R Gosnell, A.J. Taylor, J.L. Lyman, J. Chem. Phys. 94 (1991) 5949.
[6] J. van Hoeymissen, W. Uten, J. Peeters, Chem. Phys. Lett. 226 (1994) 159.
[7] M.R. Cameron, S.A. Johns, S.H. Kable, Phys. Chem. Chem. Phys. 2 (2000) 2539.
[8] M.S. Park, T.K. Kim, S.-H. Lee, K.-H. Jung, H.-R. Volpp, J. Wolfrum, J. Phys. Chem. A 105 (2001) 5606.
[9] G. Baum, P. Felder, J.R. Huber, J. Chem. Phys. 98 (1993) 1999.
[10] J.S. Guss, O. Votava, S.H. Kable, J. Chem. Phys. 115 (2001) 11118.
[11] T.W. Schmidt, G.B. Bacskay, S.H. Kable, J. Chem. Phys. 110 (1999) 11277.
[12] M.R. Cameron, G.B. Bacskay, J. Phys. Chem. A 104 (2000) 11212.
[13] S.J. Paddison, E. Tschuikow-Roux, J. Phys. Chem. 102 (1998) 6191.
[14] D.A. Dixon, D. Feller, J. Phys. Chem. A 102 (1998) 8209.
[15] D.A. Dixon, D. Feller, G. Sandrone, J. Phys. Chem. A 103 (1999) 4744.
[16] D.A. Dixon, W.A. de Jong, K.A. Peterson, J.S. Francisco, J. Phys. Chem. A 106 (2002) 4725.
[17] K. Sendt, G.B. Bacskay, J. Chem. Phys. 112 (2000) 2227.
[18] L.A. Curtiss, P.C. Redfern, V. Rassolov, G. Kedziora, J.A. Pople, J. Chem. Phys. 114 (2001) 9287.
[19] L.A. Curtiss, K. Raghavachari, P.C. Redfern, V. Rassolov, J.A. Pople, J. Chem. Phys. 109 (1998) 7764.
[20] V.A. Rassolov, M.A. Ratner, J.A. Pople, P.C. Redfern, L.A. Curtiss, J. Comput. Chem. 22 (2001) 976.

[21] B.J. Duke, L. Radom, J. Chem. Phys. 109 (1998) 3352.
[22] M.J. Frisch et al., GAUSSIAN 98 (Revision A.7), Gaussian Inc., Pittsburgh, PA, 1998.
[23] M.W. Chase Jr., NIST-JANAF Thermochemical Tables, fourth ed. [J. Phys. Chem. Ref. Data Monogr. 9 (1) 1998].
[24] J.C. Poutsma, J.A. Paulino, R.R. Squires, J. Phys. Chem. A 101 (1997) 5327.
[25] K.C. Ferguson, E. Whittle, J. Chem. Soc., Faraday Trans. 68 (1972) 295.
[26] G.P. Adams, A.S. Carson, P.G. Laye, Trans. Faraday Soc. 62 (1966) 1447.
[27] L.V. Gurvich, I.V. Veyts, C.B. Alcock, Thermodynamic Properties of Individual Substances, CRC Press, Boca Raton, FL, 1994.